
**Association Between Femur Size and a Focal
Defect of the Superior Femoral Neck**

A. H. Gee, G. M. Treece, C. J. Tonkin,
D. M. Black and K. E. S. Poole

CUED/F-INFENG/TR 696

3 February 2015

Cambridge University Engineering Department
Trumpington Street
Cambridge CB2 1PZ
England

Corresponding e-mail: ahg@eng.cam.ac.uk

Abstract

Within each sex, there is an association between hip fracture risk and the size of the proximal femur, with larger femurs apparently more susceptible to fracture. Here, we investigate whether the thickness and density of the femoral cortex play a role in this association: do larger femurs have weaker cortices? To answer this question, we used cortical bone mapping to measure the distribution of cortical mass surface density (CMSD, mg/cm^2) in cohorts of 308 males and 150 females. Principal component analysis of the various femoral surfaces led to a measure of size that is linearly independent from shape. After mapping the data onto a canonical femur surface, we used statistical parametric mapping to identify any regions where CMSD depends on size, allowing for other confounding covariates including shape. Our principal finding was a focal patch on the superior femoral neck, where CMSD is reduced by around 1% for each 1% increase in linear size ($p < 0.000005$ in the males, $p < 0.001$ in the females). This finding appears to be consistent with models of functional adaptation, and may help with the design of interventional strategies for reducing fracture risk.

1 Introduction

The relationship between hip fracture, bone strength and the geometry of the proximal femur has been much studied but poorly understood. For the sake of concision in this short paper, we cite the review by Gregory and Aspden (2008), to which the reader may refer for an extensive bibliography. Traditionally, hip geometry has been assessed in DXA images or plain radiographs using intuitive measures such as hip axis length, femoral neck axis length, femoral neck width and neck-shaft angle. Much of the literature examining these measures appears contradictory, though the apparent differences can generally be attributed to inconsistent nomenclature, measurement techniques and outcome measures (Gregory and Aspden, 2008). There is a tendency for even greater confusion when examining geometrical measurements in combination, since the various measures tend to be correlated with each other, and the outputs of predictive models based on correlated regressors need interpreting with great care. These observations are just as valid today as they were in 2008, with Machado et al. (2014) making much the same points in the introduction to their recent paper.

Gregory and Aspden (2008) make a compelling case for a more “holistic approach”, by which “shape” is decoupled from “size” and parameterized along orthogonal vectors derived from principal component analysis of the population. This is precisely the approach we take here, using 3D shape modelling to describe the proximal femur in terms of linearly independent “size” and “shape” parameters. Specifically, we investigate how femur size affects the thickness and density of the femoral cortex, using the recently developed technique of cortical bone mapping (Treece et al., 2010, 2012; Treece and Gee, 2015). We review this technique in Section 2, where we also describe the study design and statistical methods. The study’s main results are presented in Section 3, revealing a focal defect of the superior femoral neck associated with femur size. In Section 4, we discuss some important details of the methodology and also how the results shed new light on the mechanisms by which femur size affects fracture risk. Finally, we draw some conclusions in Section 5.

2 Methods

Study design

The *Osteoporotic Fractures in Men* (MrOS) study recruited 5994 men in the USA between March 2000 and April 2002 (Blank et al., 2005; Orwoll et al., 2005). Eligible subjects from six clinical sites were 65 years of age or older, able to walk without assistance, and had not had bilateral hip replacement surgery. A randomly selected cohort of 308 individuals, all with baseline QCT scans, constitutes the male subjects in the present work. The QCT scans were performed on a variety of machines, all including a calibration phantom

	n	age (years)	weight (kg)	height (cm)
males	308	73.5 ± 5.7 (65–91)	84.3 ± 14.0 (56–125)	174.3 ± 7.2 (147–198)
females	125	76.8 ± 7.4 (53–98)	66.4 ± 11.1 (40–96)	158.1 ± 6.7 (141–175)

Table 1: Sample size, age, weight and height for the male and female cohorts. The values are given as mean ± standard deviation (range).

(three-compartment, Image Analysis Inc., Columbia, KY, USA) for converting from Hounsfield Units to bone mineral density. A statistical analysis plan was submitted to the MrOS Publications Committee before receipt of the demographic data.

The female subjects were drawn from two retrospective case-control studies of hip fracture in women. The *Regional Thinning of the Femoral Neck Cortex in Hip Fracture* (FEMCO) study recruited 161 women in the UK, 50 of whom were healthy volunteers attending Addenbrooke’s Hospital, Cambridge. The *Study of Hip Joint in Trauma* recruited 150 women in the Czech Republic, 75 of whom were healthy volunteers attending Homolka Hospital, Prague. The QCT scans were performed on a variety of machines, all including a calibration phantom (five-compartment, Mindways Inc., Austin, TX, USA at Cambridge; two-compartment, Siemens AG, Erlangen, Germany at Prague). Combining the two sets of controls produces a sample size of 125. There was no *a priori* intention to examine this data in this study. Rather, for reasons that will be discussed in Section 4, there arose a need to validate the MrOS results, with the ancillary benefit of extending the conclusions to females. The FEMCO and Prague data was readily available to the authors, having previously been analysed in fracture case-control studies, and must therefore be viewed as a convenience sample.

Demographics for the male and female subjects can be found in Table 1. Informed consent was obtained from all participants.

Cortical bone mapping

Cortical bone mapping (Treece et al., 2010, 2012; Treece and Gee, 2015) is a novel technique that estimates the cortical thickness (CTh, cm), cortical bone mineral density (CBMD, mg/cm³) and cortical mass surface density (CMSD = CTh × CBMD, mg/cm²) at thousands of locations distributed over the proximal femoral surface. The most accurate and precise estimates are for CMSD (Treece and Gee, 2015), which is one of the reasons why we focus on this parameter in the present work. The other reason is that it is likely to play a significant role in local fracture resistance, accounting as it does for both the amount of cortex (CTh) and the mineralization of said cortex (CBMD).

An overview of the cortical bone mapping process can be found in Figure 1. The starting point is an approximate segmentation of the proximal femur, represented by a triangular mesh with $\sim 10^4$ vertices (Figure 1, step 1). At each vertex, the CT data is sampled along a line passing perpendicularly through the cortex (step 2). A model (step 3, red straight lines), that accounts for the imaging blur, is fitted to the data (step 3, cyan curve) so as to minimize the differences between the blurred model (step 3, red curve) and the data. This is repeated at all vertices: the resulting distributions of CTh, CBMD and CMSD can be visualised as colour maps on the femoral surface (in step 4, pink is low CMSD while blue is high CMSD). Software to perform the initial segmentation and the cortical bone mapping is available for free download¹.

¹<http://mi.eng.cam.ac.uk/~rwp/stradwin>

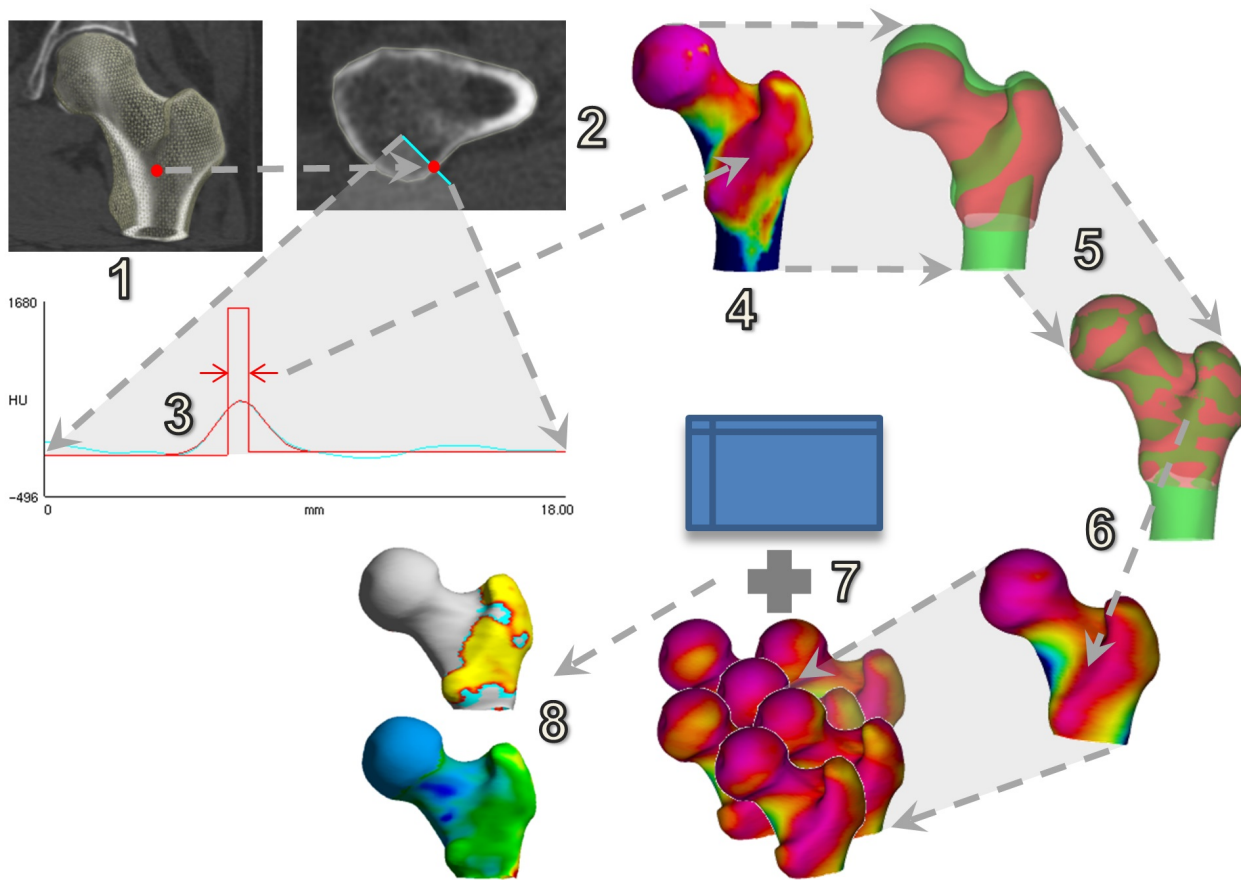


Figure 1: Cortical bone mapping (1–4), spatial registration (5–6) and statistical parametric mapping (7–8).

Statistical methods

For a cohort of size n , cortical bone mapping results in n spatial distributions like the one in Figure 1, step 4, each expressed on a different triangular mesh (since each individual femur has a different shape and size). Before we can compare these distributions and test how they depend on various regressors, we must first express each distribution on a common mesh. To this end, a canonical femur with 5580 vertices (step 5, red) is rotated, translated and nonrigidly deformed until it aligns with each individual femur (step 5, green). Once aligned, the surface data is mapped from the individual to the canonical femur and smoothed (step 6). The canonical surface mesh (which was constructed by averaging the shapes of several hundred individuals), and software to perform the registration, mapping and smoothing, are available for free download².

Following registration, we used principal component analysis to build a point-based, statistical shape model from the n sets of canonical vertex coordinates obtained by applying the n nonrigid deformations. Let \mathbf{X}_i be the 16740-element vector formed by concatenating the canonical vertex coordinates following registration with individual i , and let $\hat{\mathbf{X}} = \frac{1}{n} \sum_{i=1}^n \mathbf{X}_i$. Then the principal modes of shape variation are the eigenvectors \mathbf{m}_i of the sample covariance matrix $\frac{1}{n-1} \sum_{i=1}^n (\mathbf{X}_i - \hat{\mathbf{X}})(\mathbf{X}_i - \hat{\mathbf{X}})^T$. The first three shape modes for the two cohorts are shown in Figure 2. Shape models of this nature are the standard way to obtain compact shape descriptors of individual femurs, which may be represented according to $\mathbf{X}_i \approx \hat{\mathbf{X}} + \sum_{i=0}^k S_i \mathbf{m}_i$. For

²<http://mi.eng.cam.ac.uk/~ahg/wxRegSurf>

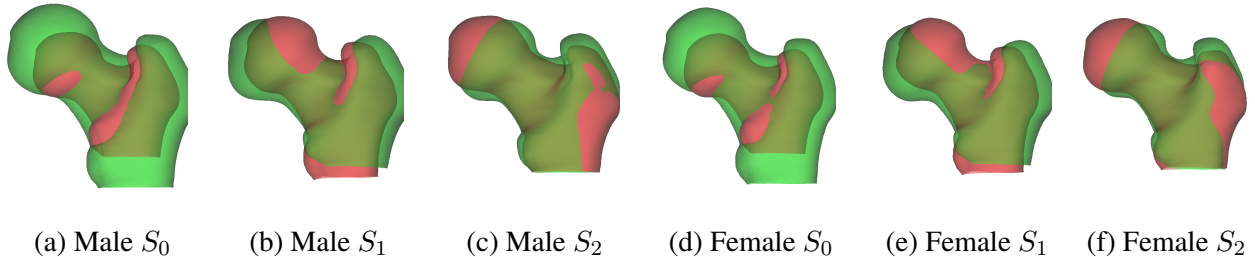


Figure 2: The first three modes of the statistical shape models, ± 3 standard deviations, accounting for 79% of the population variance in each cohort. Green is $+3$ standard deviations, red is -3 standard deviations.

	CMSD effect (% per s.d.)	CTh effect (% per s.d.)	CBMD effect (% per s.d.)
males	-6.87	-6.74	+0.07
females	-6.74	-4.90	-1.86

Table 2: Average percentage change in CMSD, CTh and CBMD per standard deviation increase in S_0 , within the default femoral neck patch.

example, setting $k = 2$ would produce a 3-element shape vector $[S_0 S_1 S_2]$ accounting for 79% of the shape variation observed in the two populations. It is apparent that S_0 corresponds roughly to femur size, S_1 to neck-shaft angle and S_2 to femoral neck axis length.

Finally, we used statistical parametric mapping (SPM) (Friston et al., 1994), as implemented in the SurfStat package (Worsley et al., 2009), to fit a general linear model (GLM) to the n sets of registered data (Figure 1, step 7), the aim being to explain the data at each vertex in terms of covariates of interest (e.g. S_0) and also confounding covariates (e.g. age, scanning site). F or t -statistics can be calculated at each vertex, to test whether the data depends significantly on the covariates, with random field theory furnishing the corresponding p -values, corrected for multiple comparisons to control the overall image-wise chance of false positives (step 8). We fitted the GLM $1 + S_0 + \text{Age} + \sum_{i=1}^5 S_i + \text{Site}$ and then performed an F -test on S_0 , to test whether CMSD depends on femur size³. In selecting this model, we anticipated age and scanning site to be confounding variables, and also allowed for nonrigid shape variation ($S_1 \dots S_5$) in order to guard against false inference caused by systematic misregistration (Gee and Treece, 2014). We performed a limited amount of data exploration to arrive at this model, with implications for statistical inference, as discussed in Section 4.

3 Results

Figure 3 shows the results of the SPM analyses on the male and female cohorts. Immediately apparent is a highly significant cluster at the superior femoral neck ($p < 0.000005$ in the males, $p < 0.001$ in the females), where CMSD decreases with increased femur size. For consistency and ease of comparison, we need to establish a specific region on the femoral neck for quantification of the S_0 effect, and we choose for this purpose the male cluster in Figure 3(b), which we henceforth refer to as the *default femoral neck patch*. Within this patch, Table 2 compares the CMSD effect with corresponding values for CTh and CBMD, derived

³For concision, and in common with many statistics packages, we use the model formula to specify the independent variables in the GLM. A model formula of the form $1 + \sum_{i=1}^5 S_i$ implies the GLM $y_j = \beta_{0,j} + \sum_{i=1}^5 \beta_{i,j} S_i + \epsilon_j$, where y_j is the dependent data (in this case, CMSD) at vertex j , $\beta_{i,j}$ are the model coefficients and ϵ_j is the residual error.

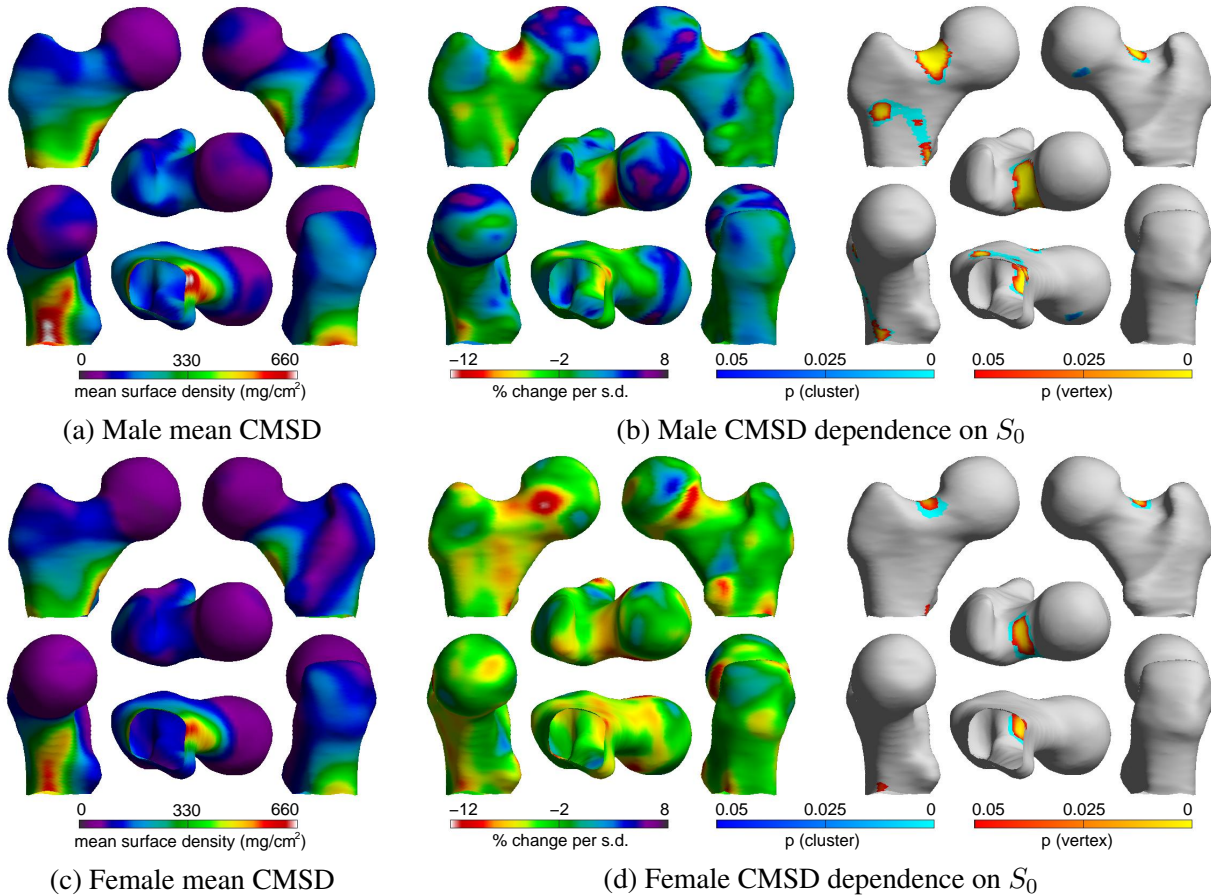


Figure 3: SPM analysis of the relationship between CMSD and femur size. The GLM fitted was $1 + S_0 + \text{Age} + \sum_{i=1}^5 S_i + \text{Site}$. The percentage change maps are derived from the S_0 coefficient in the GLM: they show the percentage change in CMSD per standard deviation increase in S_0 . The corresponding p -maps are for F -tests on S_0 . The p -maps are based on the magnitudes of vertex peaks (yellow-orange colour map, sensitive to focal effects) and on the extent of connected clusters exceeding an uncorrected p -value threshold of 0.001 (cyan-blue colour map, sensitive to distributed effects).

by fitting the same GLM to the cortical thickness and cortical bone mineral density data. Table 3 discloses the full extent of the data exploration that led to this particular statistical analysis.

4 Discussion

Magnitude and nature of the effect

The values in Table 2 indicate an average 7% reduction in CMSD, within the default femoral neck patch, per standard deviation increase in S_0 , in both the male and female cohorts. Coincidentally, one standard deviation of S_0 corresponds to an approximately 7% change in linear size, so the effect amounts to a 1% reduction in CMSD per 1% increase in linear size. As previously mentioned, CTh and CBMD estimates are less precise than those for CMSD, CTh slightly so, CBMD very significantly so (Treece and Gee, 2015). Nevertheless, the values in Table 2 are strongly suggestive of an effect that is rooted in cortical thickness, with cortical bone mineral density playing a lesser role. In Figure 3 and Table 3, the different extents, and thus significances, of

	GLM for cortical mass surface density	contrast	p (cluster)	extent (vertices)	effect (% per s.d.)
exploration n=308 males	1 + Hgt + Age + Wgt + Shp + Site*	Hgt*	2.20×10^{-2}	40	-3.50
	1 + S_0 + Age + Wgt + Shp + Site	S_0	5.09×10^{-7}	208	-7.84
	1 + S_0 + Age + Shp + Site [†]	S_0 [†]	1.15×10^{-6}	195	-6.87
confirmation n=125 females	1 + S_0 + Age + Shp + Site [†]	S_0 [†]	8.51×10^{-4}	89	-6.74

Table 3: Characteristics of the femoral neck cluster for various models and cohorts. The rightmost column quantifies the effect within the default femoral neck patch. The *a priori* analysis plan is marked *, while the final selected model is marked [†].

the male and female clusters can be attributed to the different sample sizes.

Model selection

The *a priori* MrOS analysis plan, marked * in Table 3, was to investigate how the cortex depends on the subject’s height, allowing for age, weight, shape and site. We anticipated a strong correlation between height and S_0 — the actual correlation coefficient turned out to be 0.64 — and accordingly took care not to include both in the GLM, since SPM has no way of knowing which of any correlated regressors to attribute any shared variance to. We chose to model height, since it is the more convenient parameter to measure in practice.

The *a priori* analysis plan did indeed reveal a significant association between CMSD and height at the superior femoral neck, but *post hoc* data exploration revealed the true dependency to be with femur size, S_0 : compare the cluster extents and p -values in the first two rows of Table 3. Furthermore, while the model including weight explained the data very well, it revealed an unsurprising increase in CMSD with weight over almost all of the proximal femur. Heavier males tend to have larger femurs (correlation coefficient 0.42 in the MrOS cohort), so the highly significant effect in the second row of Table 3 needs careful interpretation. The 7.84% reduction in CMSD with S_0 goes hand in hand with an increase in CMSD with weight, so it is difficult, with this particular model, to say whether larger bones do actually have reduced CMSD in the superior femoral cortex. That they do is revealed only in the final selected model, marked [†] in Table 3. This is a very clean model, with no significant correlations between the covariates, the largest correlation coefficient being -0.24 between age and one of the site labels.

SPM p -maps are corrected for multiple comparisons over vertices, but not for multiple comparisons over different GLMs and contrasts. While data exploration is undoubtedly a valuable tool at the researcher’s disposal, it must be accounted for when making claims of statistical significance, either by changing the test (e.g. Bonferroni correction, Scheffé’s method) or by confirming the findings in an independent data set. The S_0 effect in the selected model easily survives a conservative Bonferroni correction and is confirmed in the independent analysis of 125 females.

Femur size, functional adaptation and fracture risk

One of the findings that does emerge clearly from the literature is an undisputed link between increased femur size (as measured by hip axis length in particular, but other “size” metrics too) and increased fracture risk (Gregory and Aspden, 2008). There is also some consensus that cervical fractures are more strongly associated with femur size than are trochanteric fractures (Gregory and Aspden, 2008). Rivadeneira et al.

(2007) observed a link between femoral neck width and fracture risk, and went as far as to suggest that “the only reason why a wider bone would not be stronger is if cortical dimensions were thinned to the point where bone strength is lost because of instability.” Our findings sit very comfortably alongside this existing body of work. We have previously observed a focal femoral neck defect in the contralateral hip of cervical fracture cases (Poole et al., 2012), and here we show how the defect is associated with increased femur size.

Our observations appear to be quite distinct from the well known phenomenon of age-related periosteal expansion, which also leads to cortical thinning at the femoral neck associated with an enlarged femur (Beck et al., 2000). S_0 and age were uncorrelated in our studies (correlation coefficients of -0.018 in the males and 0.0031 in the females). It would seem, therefore, that we are observing a primary, spatial dependence of bone mass distribution on proximal femur geometry, rather than a secondary, temporal ageing effect. Because bone in the proximal femur is strongly influenced by functional adaptation to the prevalent loads, it is conceivable that focal osteoporosis of the superior femoral neck is a consequence of an individual’s given femoral geometry, coupled with a lifetime of bone loss in stress-shielded regions (Mayhew et al., 2005).

Femoral size has only recently been tested in simulations of functional adaptation, albeit indirectly. Models developed by Machado et al. (2014) predicted two opposing size effects: a marked decrease in femoral neck BMD with increasing femoral neck width, and a small increase in femoral neck BMD with increasing femoral neck length⁴. Since the width effect was approximately an order of magnitude greater than the length effect, our observations are entirely consistent with this model. Further analysis of our results in Appendix A confirms that the femoral neck defect is indeed amplified in wide necks and attenuated in long necks. Machado et al. (2014) also “verified that wider femoral necks present proportionally lesser BMD at the superolateral region of the neck comparatively to the inferomedial region”. All in all, there is a remarkable synergy between our observations and the functional adaptation models of Machado et al. (2014).

There are other ways of understanding how mechanical adaptation of adult bone might be influenced by femur size. Following Lovejoy’s interpretation of Frost’s mechanostat (Lovejoy, 2005), one could hypothesise that larger femurs have a greater amount of superior femoral neck bone tissue below the “trivial loading zone” that leads to bone removal though remodelling. Recent insights into bone adaptation through computer simulated dynamic mechanotransduction support this notion. Specifically, when micro-finite element models of the femur are subjected to walking simulations, the resultant femoral coronal sections show a startling similarity to true bone microstructure, with the bone tissue aligned along force trajectories at the expense of a large deficit at the superior femoral neck (Jang and Kim, 2010). We hypothesise that this bone tissue deficit would be more extensive in larger femurs. Such biomechanically driven remodelling is believed to increase bending resistance while maintaining skeletal lightness (Seeman, 2002). Currey et al. (2007) argue that functional adaptation of this nature is mainly beneficial in young adulthood during an individual’s reproductive and most physically demanding years, well before fragility sets in.

The traditional explanation of the link between hip axis length and fracture risk is that larger bones create a greater bending moment in the femoral neck during a fall (Gregory and Aspden, 2008). We suggest that the distribution of cortical bone at the superior femoral neck may also play an important role, at least when the neck is wide as well as long, as is generally the case. From a clinical perspective, while there are no practical interventions that might reduce the size of an individual’s femur, a focal femoral neck defect can potentially be addressed through targeted exercise (Allison et al., 2013) or drugs (Poole et al., 2011, 2015).

⁴ Machado et al. (2014) also considered an adjusted model to account for increased loading on very long femoral necks, and this model predicted a greater increase in BMD with neck length. For an isotropically expanding femur, the combined width and length effects sum to a $-1.4\%/+0.3\%$ change in femoral neck BMD per 1% increase in linear size for the standard/very-long-neck models.

5 Conclusions

Traditional hip structure analysis is muddled by the interdependence of the various, intuitive measures used to characterize the geometry of the proximal femur. In this work, we have instead parameterized femoral size and shape along orthogonal vectors derived from principal component analysis of the population. Our main finding was a focal defect of the superior femoral neck associated with increased femur size. The defect appears to be consistent with models of functional adaptation, and may help explain previously observed links between femur size and fracture risk, as well as inform interventional strategies for reducing that risk.

Acknowledgments

The authors thank Dr. Jan Štěpán, Charles University and Institute of Rheumatology, Prague, for providing the *Study of Hip Joint in Trauma* data. KESP acknowledges the support of the NIHR Biomedical Research Centre, Cambridge, and funding from Arthritis Research UK (reference 20109). The MrOS study is supported by National Institutes of Health (NIH) funding. The following institutes provide support: the National Institute on Aging, the National Institute of Arthritis and Musculoskeletal and Skin Diseases, the National Center for Advancing Translational Sciences and the NIH Roadmap for Medical Research, under the following grant numbers: U01 AG027810, U01 AG042124, U01 AG042139, U01 AG042140, U01 AG042143, U01 AG042145, U01 AG042168, U01 AR066160 and UL1 TR000128.

References

- Allison, S. J., Folland, J. P., Rennie, W. J., Summers, G. D., Brooke-Wavell, K., 2013. High impact exercise increased femoral neck bone mineral density in older men: A randomised unilateral intervention. *Bone* 53 (2), 321–328.
- Beck, T. J., Looker, A. C., Ruff, C. B., Sievanen, H., Wahner, H. W., Dec. 2000. Structural trends in the ageing femoral neck and proximal shaft: Analysis of the third national health and nutrition examination survey dual-energy X-ray absorptiometry data. *Journal of Bone and Mineral Research* 15 (12), 2297–2304.
- Blank, J. B., Cawthon, P. M., Carrion-Petersen, M. L., Harper, L., Johnson, J. P., Mitson, E., Delay, R. R., 2005. Overview of recruitment for the osteoporotic fractures in men study (MrOS). *Contemporary Clinical Trials* 26 (5), 557–568.
- Currey, J. D., Pitchford, J. W., Baxter, P. D., Feb. 2007. Variability of the mechanical properties of bone, and its evolutionary consequences. *Journal of the Royal Society Interface* 4 (12), 127–135.
- Friston, K. J., Holmes, A. P., Worsley, K. J., Poline, J.-P., Frith, C. D., Frackowiak, R. S. J., 1994. Statistical parametric maps in functional imaging: A general linear approach. *Human Brain Mapping* 2 (4), 189–210.
- Gee, A. H., Treece, G. M., Feb. 2014. Systematic misregistration and the statistical analysis of surface data. *Medical Image Analysis* 18 (2), 385–393.
- Gregory, J. S., Aspden, R. M., Dec. 2008. Femoral geometry as a risk factor for osteoporotic hip fracture in men and women. *Medical Engineering & Physics* 30 (10), 1275–1286.
- Jang, I. G., Kim, I. Y., Jan. 2010. Computational simulation of simultaneous cortical and trabecular bone change in human proximal femur during bone remodeling. *Journal of Biomechanics* 43 (2), 294–301.

- Lovejoy, C. O., Jan. 2005. The natural history of human gait and posture: Part 2. Hip and thigh. *Gait & Posture* 21 (1), 113–124.
- Machado, M. M., Fernandes, P. R., Zymbal, V., Baptista, F., Oct. 2014. Human proximal femur bone adaptation to variations in hip geometry. *Bone* 67, 193–199.
- Mayhew, P. M., Thomas, C. D., Clement, J. G., Loveridge, N., Beck, T. J., Bonfield, W., Burgoyne, C. J., Reeve, J., 2005. Relation between age, femoral neck cortical stability, and hip fracture risk. *The Lancet* 366 (9480), 129–135.
- Orwoll, E., Blank, J. B., Barrett-Connor, E., Cauley, J., Cummings, S., Ensrud, K., Lewis, C., Cawthon, P. M., Marcus, R., Marshall, L. M., McGowan, J., Phipps, K., Sherman, S., Stefanick, M. L., Stone, K., 2005. Design and baseline characteristics of the osteoporotic fractures in men (MrOS) study — a large observational study of the determinants of fracture in older men. *Contemporary Clinical Trials* 26 (5), 569–585.
- Poole, K. E., Treece, G. M., Gee, A. H., Brown, J. P., McClung, M. R., Wang, A., Libanati, C., 2015. Denosumab rapidly increases cortical bone in key locations of the femur: A 3D bone mapping study in women with osteoporosis. *Journal of Bone and Mineral Research* 30 (1), 46–54.
- Poole, K. E. S., Treece, G. M., Mayhew, P. M., Vaculik, J., Dungal, P., Horák, M., Štěpán, J. J., 2012. Cortical thickness mapping to identify focal osteoporosis in patients with hip fracture. *PLoS ONE* 7 (6), e38466.
- Poole, K. E. S., Treece, G. M., Ridgway, G. R., Mayhew, P. M., Borggrefe, J., Gee, A. H., 2011. Targeted regeneration of bone in the osteoporotic human femur. *PLoS ONE* 6 (1), e16190.
- Rivadeneira, F., Zillikens, M. C., Laet, C. E. D. H. D., Hofman, A., Uitterlinden, A. G., Beck, T. J., Pols, H. A. P., Nov. 2007. Femoral neck BMD is a strong predictor of hip fracture susceptibility in elderly men and women because it detects cortical bone instability: The Rotterdam study. *Journal of Bone and Mineral Research* 22 (11), 1781–1790.
- Seeman, E., May 2002. Pathogenesis of bone fragility in women and men. *The Lancet* 359 (9320), 1841–1850.
- Treece, G. M., Gee, A. H., Feb. 2015. Independent measurement of femoral cortical thickness and cortical bone density using clinical CT. *Medical Image Analysis* 20 (1), 249–264.
- Treece, G. M., Gee, A. H., Mayhew, P. M., Poole, K. E. S., Jun. 2010. High resolution cortical bone thickness measurement from clinical CT data. *Medical Image Analysis* 14 (3), 276–290.
- Treece, G. M., Poole, K. E. S., Gee, A. H., Jul. 2012. Imaging the femoral cortex: thickness, density and mass from clinical CT. *Medical Image Analysis* 16 (5), 952–965.
- Worsley, K., Taylor, J., Carbonell, F., Chung, M., Duerden, E., Bernhardt, B., Lyttelton, O., Boucher, M., Evans, A., 2009. SurfStat: A Matlab toolbox for the statistical analysis of univariate and multivariate surface and volumetric data using linear mixed effects models and random field theory. *NeuroImage* 47 (Supplement 1), S102–S102, Organization for Human Brain Mapping, 2009 Annual Meeting.

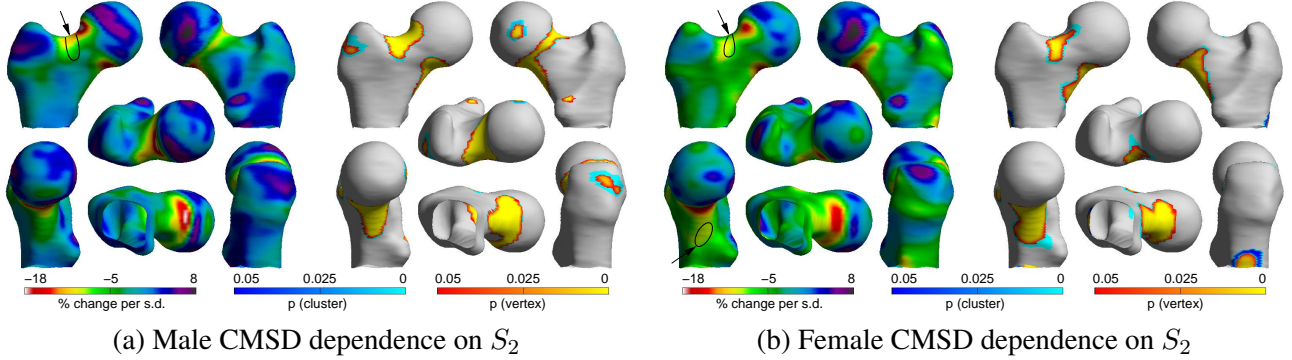


Figure 4: SPM analysis of the relationship between CMSD and S_2 . The GLM fitted was $1 + S_0 + \text{Age} + \sum_{i=1}^5 S_i + \text{Site}$. The percentage change maps are derived from the S_2 coefficient in the GLM: they show the percentage change in CMSD per standard deviation increase in S_2 . The corresponding p -maps are for F -tests on S_2 . The arrows indicate regions where the effects cannot be attributed to systematic misregistration.

A The effect of S_2 on cortical mass surface density

The models of functional adaptation in Machado et al. (2014) predict dramatically reduced femoral neck BMD with wider femoral necks, but slightly increased BMD with longer femoral necks. While this is consistent with our main finding for overall femur “size”, it does beg the question as to whether we can detect the opposing width-length effects in the CT data. We therefore undertook a tentative investigation of S_2 , which corresponds roughly to femoral neck axis length (see Figure 2).

SPM analyses of dependencies on S_i ($i > 0$) are challenging, because it is difficult to disentangle true effects from inevitable misregistration artefacts. Femurs with a large S_1 tend to register with the canonical femur one way, those with a small S_1 another way, and likewise with the other shape modes. Consequently, each individual’s cortical distribution “slips” around the canonical surface in a manner that depends on shape, and the resulting artefactual variation may be incorrectly interpreted as a true effect (Gee and Treece, 2014).

Proceeding, then, with due caution, Figure 4 suggests that CMSD might depend on S_2 in both the male and female cohorts. A scale-comparison heuristic (Gee and Treece, 2014) reveals that most of the significant clusters can in fact be explained by systematic misregistration, apart from at the small regions indicated by arrows. There does, therefore, appear to be a genuine dependence of CMSD on S_2 at the superior femoral neck. Larger values of S_2 (shorter, wider necks) are associated with less CMSD, whereas smaller values of S_2 (longer, thinner necks) are associated with more CMSD. This is consistent with the modelling in Machado et al. (2014).